Nanopatterned aluminum nitride template for high efficiency light-emitting diodes

Sang-Mook Kim[1,2], Tae-Young Park[1], Seong-Ju Park[1], Seung-Jae Lee[2], Jong Hyeob Baek[2], Yun Chang Park[3], and Gun Young Jung[1,*]

[1]*Department of Materials Science and Engineering, Gwangju Institute of Science and Technology (GIST), 1 Oryong-dong, Buk-gu, Gwangju 500-712, Republic of Korea*

[2] *Korea Photonics Technology Institute (KOPTI), Gwangju, Korea, 971-3 Wouchul-Dong, Buk-gu, Gwangju 500-460, Republic of Korea*

[3]*Measurements and Analysis Division, National NanoFab Center (NNFC) 335, Gwahangno, Yuseong-gu, Daejeon, 305-806, Republic of Korea*

** gyjung@gist.ac.kr*

Abstract: Nanopatterned aluminum nitride (NP-AlN) templates were used to enhance the light extraction efficiency of the light-emitting diodes (LEDs). Here, the NP-AlN interlayer between the sapphire substrate and GaN-based LED was used as an effective light outcoupling layer at the direction of bottom side and as a buffer layer for growth of GaN LEDs. The cross-sectional transmission electron microscopy (TEM) analysis showed that the formation of stacking faults and voids could help reduce the threading dislocations. Micro Raman spectra also revealed that the GaN-based epilayer grown on the NP-AlN template had smaller residual stress than that grown on a planar sapphire substrate. The normalized electroluminescence (EL) spectra at the top and bottom sides of device revealed that the enhancement of the bottom side emission of the LED with the NP-AlN interlayer was more notable than a planar sapphire substrate due to the graded-refractive-index (GRIN) effect of the NP-AlN.

OCIS codes: (230.0250) Optoelectronics; (230.3670) Light-emitting diodes; (220.4241) nanostructure fabrication; (110.4235) Nanolithography; (290.5880) Scattering, rough surfaces; (170.5660) Raman spectroscopy; (310.6860) Thin films, optical properties

References and links

1. D. Xiao, K. W. Kim, S. M. Bedair, and J. M. Zavada, "Design of white light-emitting diodes using InGaN/AlInGaN quantum-well structures," Appl. Phys. Lett. **84**(5), 672–674 (2004).
2. D.-Y. Kang, E. Wu, and D.-M. Wang, "Modeling white light-emitting diodes with phosphor layers," Appl. Phys. Lett. **89**(23), 231102 (2006).
3. J. K. Sheu, C. J. Pen, G. C. Chi, C. H. Kuo, L. W. Wu, C. Chen, H. Chang, and Y. K. Su, "White-light emission from InGaN-GaN multi quantum-well light-emitting diodes with Si and Zn codoped active well layer," IEEE Photon. Technol. Lett. **14**(4), 450–452 (2002).
4. I. Schnitzer, E. Yablonovitch, C. Caneau, T. J. Gmitter, and A. Scherer, "30% external quantum efficiency from surface textured, thin-film light-emitting diodes," Appl. Phys. Lett. **63**(16), 2174–2176 (1993).
5. H.-W. Huang, C. C. Kao, J. T. Chu, H. C. Kuo, S. C. Wang, and C. C. Yu, "Improvement of InGaN-GaN light-emitting diode performance with a nano-roughened p-GaN surface," IEEE Photon. Technol. Lett. **17**(5), 983–985 (2005).
6. K. Tadatomo, H. Okagawa, Y. Ohuchi, T. Tsunekawa, Y. Imada, M. Kato, and T. Taguchi, "High output power InGaN ultraviolet light-emitting diodes fabricated on patterned substrates using metalorganic vapor phase epitaxy," Jpn. J. Appl. Phys. **40**(Part 2, No. 6B), L583–L585 (2001).
7. T.-X. Lee, K.-F. Gao, W.-T. Chien, and C.-C. Sun, "Light extraction analysis of GaN-based light-emitting diodes with surface texture and/or patterned substrate," Opt. Express **15**(11), 6670–6676 (2007).
8. J. J. Wierer, M. R. Krames, J. E. Epler, N. F. Gardner, M. G. Craford, J. R. Wendt, J. A. Simmons, and M. M. Sigalas, "InGaN/GaN quantum-well heterostructure light-emitting diodes employing photonic crystal structures," Appl. Phys. Lett. **84**(19), 3885–3887 (2004).
9. C. H. Chiu, H. H. Yen, C. L. Chao, Z. Y. Li, Yu. Peichen, H. C. Kuo, T. C. Lu, S. C. Wang, K. M. Lau, and S. J. Cheng, "Nanoscale epitaxial lateral overgrowth of GaN-based light-emitting diodes on a SiO2 nanorod-array patterned sapphire template," Appl. Phys. Lett. **93**(8), 081108 (2008).

#113564 - $15.00 USD Received 1 Jul 2009; revised 30 Jul 2009; accepted 31 Jul 2009; published 5 Aug 2009

10. J. K. Kim, A. N. Noemaun, F. W. Mont, D. Meyaard, E. F. Schubert, D. J. Poxson, H. Kim, C. Sone, and Y. Park, "Elimination of total internal reflection in GaInN light-emitting diodes by graded-refractive-index micropillars," Appl. Phys. Lett. **93**(22), 221111 (2008).
11. L. W. Sang, Z. X. Qin, H. Fang, T. Dai, Z. J. Yang, B. Shen, G. Y. Zhang, X. P. Zhang, J. Xu, and D. P. Yu, "Reduction in threading dislocation densities in AlN epilayer by introducing a pulsed atomic-layer epitaxial buffer layer," Appl. Phys. Lett. **93**(12), 122104 (2008).
12. G.-Y. Jung, E. Johnston-Halperin, W. Wu, Z. Yu, S.-Y. Wang, W. M. Tong, Z. Li, J. E. Green, B. A. Sheriff, A. Boukai, Y. Bunimovich, J. R. Heath, and R. S. Williams, "Circuit Fabrication at 17 nm Half-Pitch by Nanoimprint Lithography," Nano Lett. **6**, 351–354, (2006).
13. H. K. Cho, J. Y. Lee, K. S. Kim, G. M. Yang, J. H. Song, and P. W. Yu, "Effect of buffer layers and stacking faults on the reduction of threading dislocation density in GaN overlayers grown by metalorganic chemical vapor deposition," J. Appl. Phys. **89**(5), 2617 (2001).
14. K. Dovidenko, S. Oktyabrsky, J. Narayan, and M. Razeghi, "Aluminum nitride films on different orientations of sapphire and silicon," J. Appl. Phys. **79**(5), 2439–2445 (1996).
15. Y. D. Wang, K. Y. Zang, S. J. Chua, S. Tripathy, P. Chen, and C. G. Fonstad, "Nanoair-bridged lateral overgrowth of GaN on ordered nanoporous GaN template," Appl. Phys. Lett. **87**(25), 251915 (2005).
16. P. Puech, F. Demangeot, J. Frandon, C. Pinquier, M. Kuball, V. Domnich, and Y. Gogotsi, "GaN nanoindentation: A micro-Raman spectroscopy study of local strain fields," J. Appl. Phys. **96**(5), 2853–2856 (2004).
17. V. Lughi, and D. R. Clarke, "Defect and stress characterization of AlN films by Raman spectroscopy," Appl. Phys. Lett. **89**(24), 241911 (2006).
18. C.-C. Chen, C.-C. Yeh, C.-H. Chen, M.-Y. Yu, H.-L. Liu, J.-J. Wu, K.-H. Chen, L.-C. Chen, J.-Y. Peng, and Y.-F. Chen, "Catalytic growth and characterization of gallium nitride nanowires," J. Am. Chem. Soc. **123**(12), 2791–2798 (2001).
19. H. K. Cho, J. Jang, J. H. Choi, J. Choi, J. Kim, J. S. Lee, B. Lee, Y. H. Choe, K. D. Lee, S. H. Kim, K. Lee, S. K. Kim, and Y. H. Lee, "Light extraction enhancement from nano-imprinted photonic crystal GaN-based blue light-emitting diodes," Opt. Express **14**(19), 8654–8660 (2006).
20. H. Gao, F. Yan, Y. Zhang, J. Li, Y. Zeng, and G. Wang, "Fabrication of nano-patterned sapphire substrates and their application to the improvement of the performance of GaN-based LEDs," J. Phys. D Appl. Phys. **41**(11), 115106 (2008).
21. J.-H. Ryou, W. Lee, J. Limb, D. Yoo, J. P. Liu, R. D. Dupuis, Z. H. Wu, A. M. Fisher, and F. A. Ponce, "Control of quantum-confined Stark effect in InGaN/GaN multiple quantum well active region by p-type layer for III-nitride-based visible light emitting diodes," Appl. Phys. Lett. **92**(10), 101113 (2008).

1. Introduction

Light-emitting diodes (LEDs) are in high demand due to their application in the areas of signals, displays, and illumination devices [1,2]. In order to improve the external light efficiency, however, it is essential to enhance the both the extraction and internal efficiencies in LED structures [3]. Previously, enhancement of the light extraction efficiency was achieved by reducing the total internal reflection (TIR) [4]. For TIR reduction, several approaches have been proposed: surface roughening [5], GaN epilayer growth on a patterned sapphire substrate [6,7], and integration of two dimensional (2-D) photonic crystal (PC) structures [8]. Recently, incorporating geometric structures inside an LED [9] and graded-refractive-index (GRIN) pillars on the emitting surface [10] have also been reported.

In this work, we grew an aluminum nitride (AlN) template using metalorganic chemical deposition (MOCVD) and then fabricated nanopatterned (NP)-AlN structures using nanoimprint lithography (NIL). Among the III-nitride semiconductors, AlN exhibits the largest direct band gap (6.2 eV), high thermal conductivity, and a refractive index of ~2.15, which is roughly the median point between GaN (n = 2.40) and a sapphire substrate (n = 1.78). The NP-AlN interlayer between the sapphire substrate and GaN-based LEDs was used as an effective light outcoupling layer based on its characteristics as a GRIN antireflection layer as well as a buffer layer for the growth of GaN LEDs.

#113564 - $15.00 USD Received 1 Jul 2009; revised 30 Jul 2009; accepted 31 Jul 2009; published 5 Aug 2009

2. Experiments

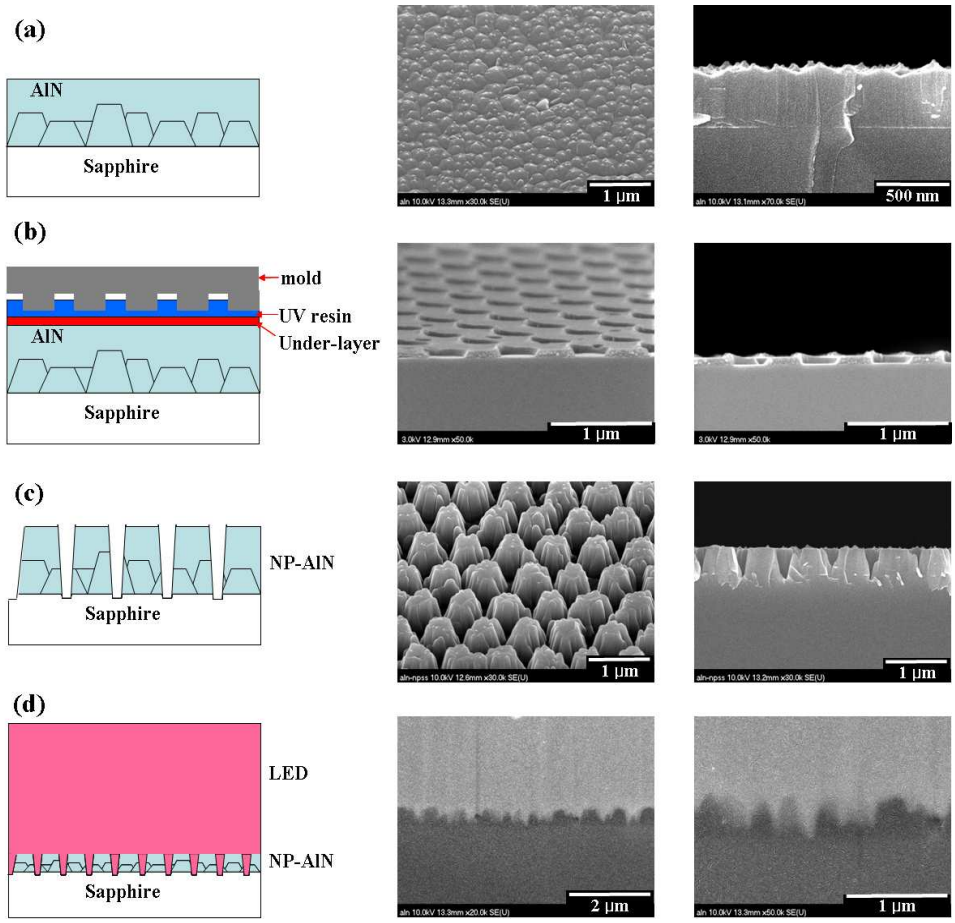

Fig. 1. Schematic diagram of process flow with corresponding SEM images: (a) 300 nm-thick AlN film grown on a *c*-face (0001) sapphire substrate, (b) fabrication of nanoscale patterns for etching masks through a bi-layer resist structure using nanoimprint lithography, (c) NP-AlN with a diameter of 500 nm, a pitch of 700 nm, and a depth of 300 nm, and (d) the blue LED grown on the NP-AlN substrate using an MOCVD system. The left SEM images are tilt view and right SEM images are cross-sectional view of (a), (b), and (c). In the case of (d), the left image is the cross-sectional view and the corresponding magnified image (right).

AlN films for this study were deposited at a 300 nm thickness on a *c*-face (0001) sapphire substrate for 3 h using an MOCVD system at a temperature of 1050 °C, a pressure of 200 torr, and a molar V/III ratio of 1800. In addition, the trimethylaluminum (TMA) and ammonia (NH_3) were used as precursors, and the carrier gas of hydrogen was kept constant at 10 SLM. Scanning electron microscopy (SEM) images [Fig. 1(a)] revealed that the AlN films consisted of a large number of hexagonal columnar grains [11].

Figure 1 illustrates the procedure for fabricating the NP-AlN template. After AlN film preparation, the NIL was used to fabricate the nanoscale patterns, and the details were previously reported [12]. Figure 1(b) shows the imprinted nanoscale patterns on top of the AlN layer through the bi-layer resist structure. An ultraviolet (UV)-curable resin was spin-coated on the sacrificial under-layer (LOL 1000, Shipley) coated sample. Then, the pillar-type glass mold was pressed at a pressure of 10 bars for 3 min and blanket UV irradiation was performed through the glass mold for 60 sec using a nanoimprint machine. After pattern replication into the imprint resist, the printed pattern was treated in a CF_4 gas plasma to remove any residual resist layer under the printed trenches. Then, oxygen plasma treatment

#113564 - $15.00 USD Received 1 Jul 2009; revised 30 Jul 2009; accepted 31 Jul 2009; published 5 Aug 2009

was carried out to transfer the pattern to the under layer of lift-off layer. Following a 20 nm thick chromium (Cr) deposition, metal lift-off process was subsequently performed by soaking the sample in a polymer remover (1165, Shipley), resulting in Cr etching masks for the next drying-etching process. The AlN layer was etched using inductively coupled plasma (ICP) etching with a gas mixture of Cl_2 and BCl_3. In this process, the sapphire substrate was shallowly etched (~50 nm) and it was helpful to increase the light scattering at the GaN/sapphire interface. Figure 1(c) shows the scanning electron microscopy (SEM) images of the NP-AlN template with a diameter of 500 nm and a center-to-center distance of 700 nm.

The conventional InGaN/GaN multiple quantum well (MQW) blue LED structures were grown simultaneously on both the NP-AlN template [Fig. 1(d)] and the planar sapphire substrate using an MOCVD system to eliminate the variation in device characteristics from wafer to wafer. From the bottom to the top, the LED structure consists of a 30 nm-thick GaN nucleation layer, a 2 μm-thick unintentionally doped GaN layer, a 1.5 μm-thick Si-doped GaN *n*-cladding layer (*n*-GaN), a region with five periods of InGaN/GaN MQWs, a 0.11 μm-thick Mg-doped GaN layer (*p*-GaN), and a 10 nm-thick Mg-doped GaN layer (p^+-GaN). Finally, LEDs (300 × 300 μm ^{2}) were fabricated and measured for the comparison of LED performance.

3. Results and discussion

3.1 Transmission electron microscopy analysis

In order to investigate the crystalline quality of GaN-based blue LEDs grown on a planar sapphire substrate and on the NP-AlN template, transmission electron microscopy (FETEM, FEI, Tecnai F30 Super-Twin) analysis was performed. Cross-sectional specimens for TEM and EDX were prepared using cutting, gluing, polishing, dimpling and ion beam milling (GATAN, PIPS 691) for electron transparency.

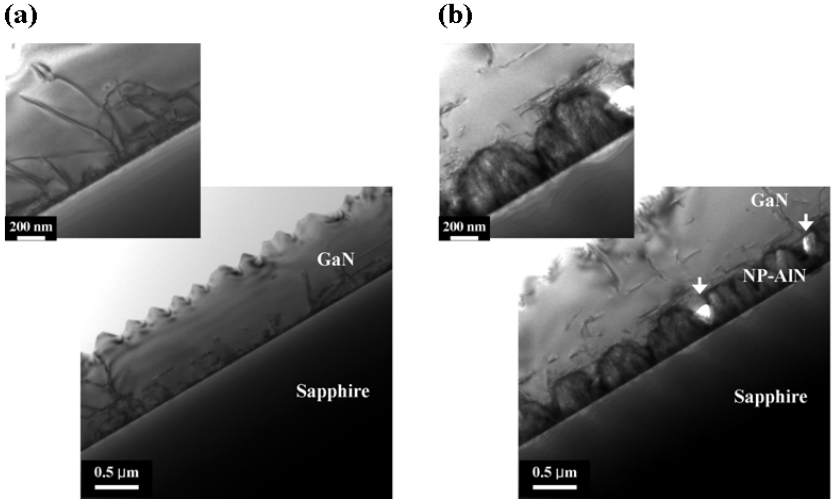

Fig. 2. Cross-sectional TEM images of the GaN epilayer grown (a) on a planar sapphire substrate and (b) on the NP-AlN template. The insets show the high-magnification images.

As shown in Figs. 2(a) and 2(b), the GaN-based epilayer grown on the NP-AlN template has better quality and crystallinity than the epilayer on planar sapphire substrate. The improved quality can be attributed to the fact that the NP-AlN template has a smaller lattice mismatch with the GaN epilayer than that of the GaN buffer layer grown directly on the planar sapphire substrate. Thus, these results clearly show that the GaN epilayer grown on the NP-AlN had more stacking faults than that grown on the planar sapphire substrate. The stacking faults, which were expected to form due to the different strains at the boundary

#113564 - $15.00 USD Received 1 Jul 2009; revised 30 Jul 2009; accepted 31 Jul 2009; published 5 Aug 2009

between the GaN epilayers grown on the sapphire and the NP-AlN template, could help reduce the threading dislocation density within the GaN epilayers. Moreover, the voids at the vicinity of the AlN rods [arrows in Fig. 2(b)] confirm the lateral growth of GaN epilayer near the edge of the AlN nanorods [9,13].

In addition, the high-resolution TEM (HRTEM) and the corresponding selected-area diffraction pattern (SADP) study were carried out for more investigation about the quality of the interface. Representative bright field TEM image [Fig. 3(a)] and corresponding selected area electron diffraction (SAED) pattern [Fig. 3(b)] projected in $[100]_{AlN}$, $[100]_{GaN}$, and $[001]_{sapphire}$ zone axis show the epitaxial growth relationship; $(001)_{GaN}//(001)_{AlN}//(001)_{sapphire}$ and $(010)_{GaN}//(010)_{AlN}//(110)_{sapphire}$. $[100]_{AlN}$ and $[100]_{GaN}$ coincided with $[1\text{–}10]_{sapphire}$ in case of 30 ° rotation to *c* axis in hexagonal system [14]. Figures 3(c) and 3(d) show the cross-sectional HRTEM images of GaN/NP-AlN/sapphire. Moire fringes (wavy form) were observed in the overlapped region of the AlN and GaN epilayer. Figure 3(d), high resolution TEM image of the area of enclosed red dotted box in Fig. 3(c), shows epitaxial GaN film with lots of planar defects (stacking faults, white arrows) parallel to (001) basal plane in the hexagonal system.

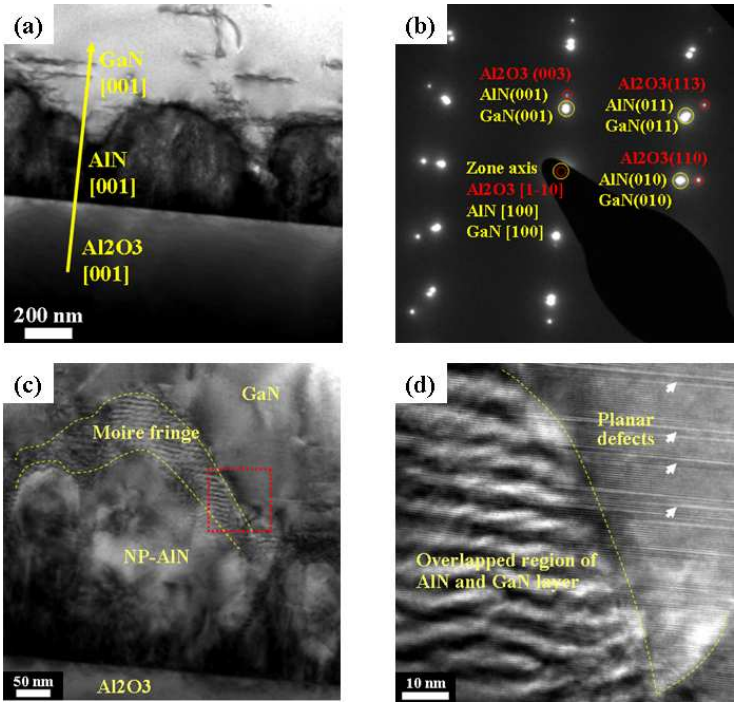

Fig. 3. (a) Representative bright field TEM image and (b) the corresponding selected area electron diffraction (SAED) pattern. (c) Bright field TEM image of a GaN on the NP-AlN and (d) high-resolution image of the red dotted box in (c).

3.2 Raman spectroscopy

Figure 4 shows the Raman scattering spectrum collected using a 514.5 nm Ar^+ laser with a power of 2.4 mW (Jobin-Yvon LabRam HR). The E_2 (high) mode peaks of the GaN layer grown on a planar sapphire substrate and the NP-AlN template were located at 568.804 and 567.826 cm^{-1}, respectively. It was previously reported that the peak of a strain-free GaN layer was about 566.5 cm^{-1} [15]; here, the shift of ~0.978 cm^{-1} towards the stress-free GaN layer in case of the NP-AlN template indicates a relaxation of the compressive stress in the overgrown GaN layer. The in-plane compressive stress could be estimated using the equation $\Delta\omega = 2.25\ \sigma$, where $\Delta\omega$ is the observed peak shift with respect to the stress-free GaN layer [16]. In this

#113564 - $15.00 USD Received 1 Jul 2009; revised 30 Jul 2009; accepted 31 Jul 2009; published 5 Aug 2009

case, the calculated stress (σ) was about 0.589 and 1.024 GPa for GaN layer with and without the NP-AlN template, respectively. The broader Raman spectra could be attributed to the different stress state in the GaN film grown on different substrate conditions (AlN and sapphire) and the phonon confinement in crystallite boundaries of nano-sized epilayers, which were grown between NP-AlNs at the bottom [17,18]. The smaller residual stress of the GaN-based LED with the NP-AlN template could greatly reduce the dislocation and thus improve the quantum efficiency.

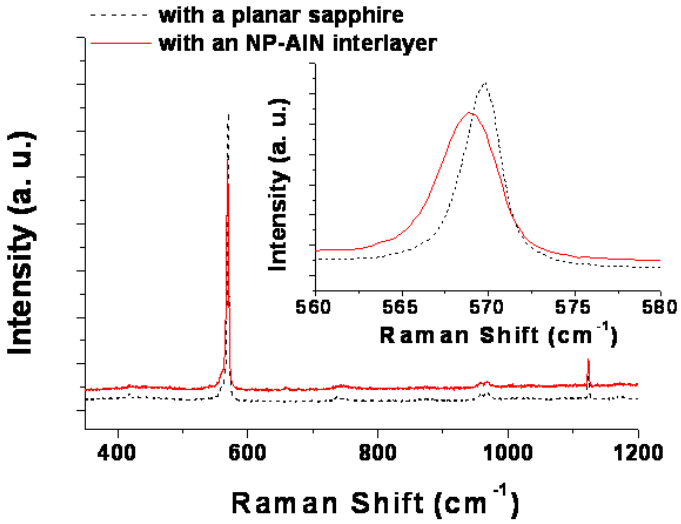

Fig. 4. Room-temperature Raman spectra of a GaN layer grown on a planar sapphire substrate and the NP-AlN. The inset shows an enlarged view of the spectral region at the *E*2 (high) optical phonon mode of the GaN epilayer.

3.3 Electroluminescence measurement at the top and the bottom

To investigate the GRIN effect of the NP-AlN interlayer between sapphire substrate and GaN-based LED, we measured the electroluminescence (EL) using an optical spectrometer and a photodiode detector located at the top and bottom of the device under an injection current of 20 mA [Fig. 5]. The EL spectra revealed that the top emission and bottom emission power of an LED having the NP-AlN interlayer increased 1.60- and 2.5-fold compared to those of a LED with a planar sapphire substrate, respectively. The enhancement of the top side emission of the LED with the NP-AlN interlayer could be explained by the following two reasons; increment of light scattering by the NP-AlN and shallow etched sapphire substrate, and improvement of quantum efficiency by reducing the dislocation. Furthermore, the notable increase of the bottom side emission of the LED with the NP-AlN interlayer is due to the GRIN effect of the NP-AlN between the sapphire substrate and the GaN-based LED.

#113564 - $15.00 USD Received 1 Jul 2009; revised 30 Jul 2009; accepted 31 Jul 2009; published 5 Aug 2009

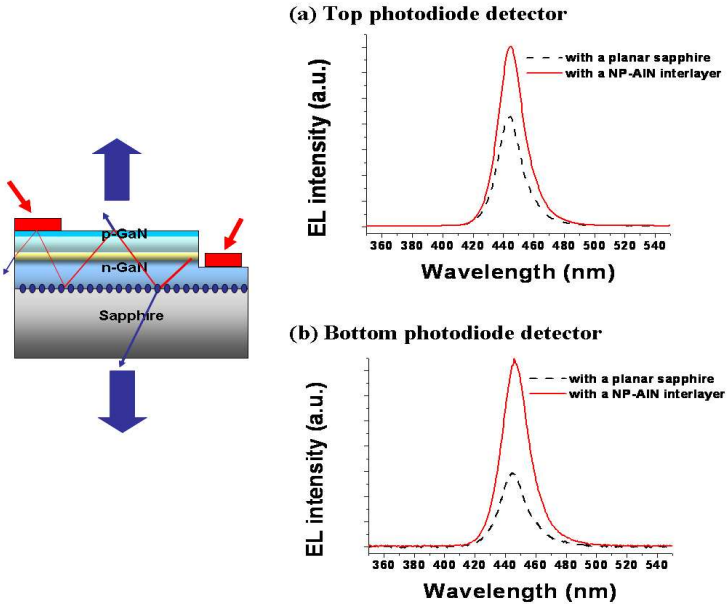

Fig. 5. The EL spectra of LEDs with and without the NP-AlN interlayer measured using the (a) top and (b) bottom photodiode detector.

3.4 3D finite difference time domain simulations

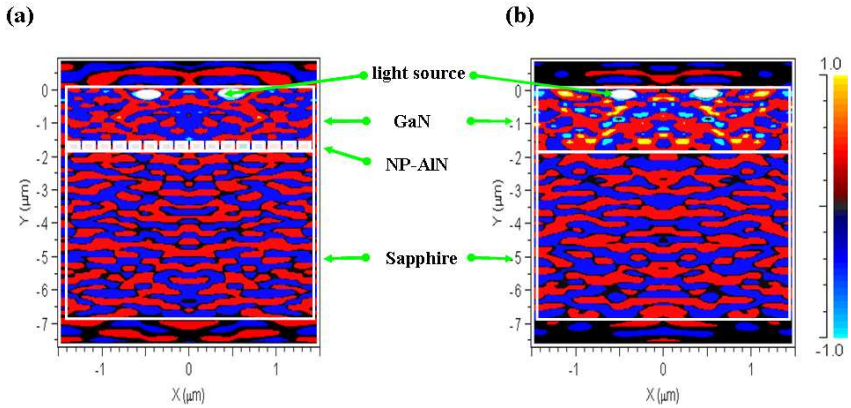

Fig. 6. 3D-FDTD simulation results of light propagation of LEDs (a) with and (b) without the NP-AlN interlayer.

In order to confirm the efficiency of our LED theoretically, the finite difference time domain (FDTD) mathematical technique was performed to compare the light extraction efficiency of the LEDs using a FullWAVE^{TM} program [19]. For the effective observation of the light propagation, we assume that the GaN LEDs are composed of a single GaN layer and a thin sapphire substrate, and have two light sources at the active region.

Figures 6(a) and (b) clearly show that the photons emitted from the LED with the NP-AlN interlayer were less trapped in the GaN layer and more propagated vertically. The LED without the NP-AlN illustrates the high intensity areas, yellow spots, trapped within the GaN slab [Fig. 6(b)]. In the case of the LED with the NP-AlN interlayer, the photons could be released to the outside of the LED without trapping in the GaN, resulting in an enhancement of light output.

#113564 - $15.00 USD Received 1 Jul 2009; revised 30 Jul 2009; accepted 31 Jul 2009; published 5 Aug 2009

3.5 L-I-V characteristics

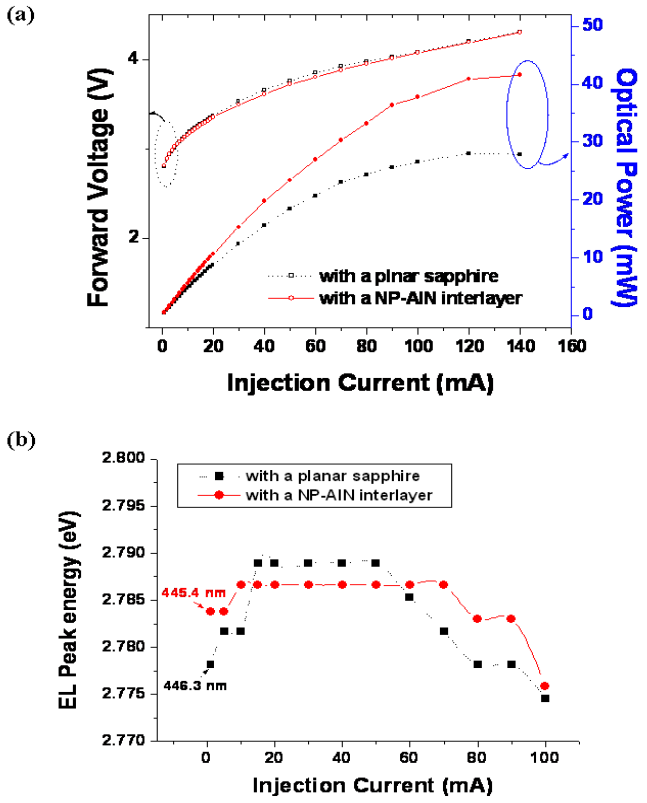

Fig. 7. (a) Room-temperature L–I–V characteristics and (b) EL peak energy as a function of injection current for LEDs with and without the NP-AlN interlayer.

For the evaluation of LED performance, LEDs were packaged on a transistor outline (TO)-18 without epoxy encapsulation. The measured light output powers are the overall value of the top and bottom side emission because the silver (Ag) epoxy for attaching the LEDs to the TO-18 reflected the light at the bottom and an integrating sphere was used as a detector system. Figure 7(a) presents the typical forward L-I-V characteristics. The light output (at 20 mA) of the LEDs with a planar sapphire substrate and the NP-AlN template was 8.8 mW and 10.7 mW, respectively. The light output power enhancement of the LED with the NP-AlN template could be explained by the GRIN effect at the bottom side and the better crystalline quality of the GaN-based blue LED. Moreover, the LED with the NP-AlN interlayer demonstrated an improved external efficiency at high current operation; it is beneficial in the aspect of device stability and efficiency droop behavior.

To confirm the relief in compressive stress of LEDs with the NP-AlN interlayer, the EL spectra under an injection current was measured [Fig. 7(b)]. When the injection current increased from 1 to 50 mA, the EL peak energy increased from 2.784 to 2.787 eV in the LED with the NP-AlN interlayer and from 2.778 to 2.789 eV in the LED with a planar sapphire, respectively. These blue-shift phenomena of the GaN-based LED could be explained by weakening the quantum confined stark effect (QCSE) due to the charge screening effect and band filling of localized states [20,21]. As such, the reduced blue-shift with increasing current for the LED with the NP-AlN may be due to a reduction in compressive strain. Note that the

#113564 - $15.00 USD Received 1 Jul 2009; revised 30 Jul 2009; accepted 31 Jul 2009; published 5 Aug 2009

red-shift in the high current region can be explained by the effect of band shrinkage due to Joule heat generation.

4. Summary

In summary, we fabricated the LEDs with and without NP-AlN interlayers and then compared their characteristics. The cross-sectional TEM micrographs and micro Raman spectra showed that the GaN-based epilayer grown on the NP-AlN template had better quality and smaller residual stress than the GaN epilayers grown on a planar sapphire substrate. The EL spectra revealed further that the top and bottom emission powers of LEDs with the NP-AlN interlayer increased 1.6- and 2.5-fold, respectively, compared to that of LEDs having a planar sapphire substrate. The FDTD simulation results clearly illustrate that the LEDs with the NP-AlN interlayer had higher light extraction efficiency than LEDs without it, due to the scattering and GRIN effect of the NP-AlN interlayer. As a result, the overall output power of the LEDs on a TO-18 package was enhanced by 21.6% compared to conventional LEDs.

Acknowledgements

This work was supported by the Korea Science and Engineering Foundation (KOSEF) NCRC grant funded by the Korea government (MEST) (No. R15-2008-006-03002-0) and the Industry Technology Development Project (No. 10032325-2008-11) funded by the Korea Ministry Knowledge and Economy (MKE).

#113564 - $15.00 USD Received 1 Jul 2009; revised 30 Jul 2009; accepted 31 Jul 2009; published 5 Aug 2009